A high active type of hydroxyapatite for photocatalytic decomposition of dimethyl sulfide under UV irradiation

Harumitsu Nishikawa

Gifu Prefectural Institute of Health and Environmental Sciences, 1-1, Naka-fudogaoka, Kakamigahara-shi, Gifu 504-0838, Japan

Abstract

A very active type of hydroxyapatite (HAp-2) for photocatalytic decomposition of dimethyl sulfide (DMS) under UV irradiation and its structural characteristics were studied. The conversion of DMS using HAp-2 was 98–100% at the space velocity of $340\,h^{-1}$ under UV irradiation, and the activity of HAp-2 was higher than that of another type of HAp (HAp-1). The photocatalytic decomposition of DMS proceeded oxidatively and effectively on HAp-2 under UV irradiation. It was recognized that DMS converted stoichiometrically to CO_2 on HAp-2. From the X-ray diffraction (XRD) studies, the HAp-1 crystals had a lower crystallinity than crystals of HAp-2 toward the apatite a-axis, but a similar crystallinity toward the c-axis. Then, it was concluded that the photocatalytic activity of HAp must be due to the crystallinity toward the a-axis of HAp crystal.
© 2003 Elsevier B.V. All rights reserved.

Keywords: Hydroxyapatite; Photocatalytic decomposition; Dimethyl sulfide; Oxygen radical

1. Introduction

Catalytic reactions of organic compounds, such as alcohol [1,2], 1-butene [3], and cyclohexanone oxime [4], and chlorobenzene [5,6] on hydroxyapatite are well known. We have reported on oxidative decomposition of gaseous chlorinated organic compounds, such as trichloroethylene and chlorobenzene, over calcium-deficient hydroxyapatite [7–10] under heating condition. Hydroxyapatite is very useful as bio- and eco-materials and very safe for human life.

Monma et al. investigated the radical formation on non-stoichiometric hydroxyapatite above 473 K, and the radical was assumed to be due to electrons trapped in a strained structure [11]. Recently, Kanai and co-workers have reported on the activation of stoichiometric hydroxyapatite (HAp) by heat treatment or UV irradiation and on the formation of radical species, such as O_3^- species from UV irradiation [12,13]. Electron spin resonance (ESR) studies of radical species in X-ray or γ-ray-irradiated HAp were also reported by Moens and co-workers [14–16], Schramm and Rossi [17,18] and Murata et al. [19]. The radical formation on HAp under UV irradiation must be different from that under the higher energy irradiation, such as X-ray or γ-ray.

We have reported on thermal behavior of HAp in structural and spectrophotometric characteristics [20], and also found the photocatalytic decomposition of methyl mercaptane (MM) over HAp under UV irradiation in the previous paper [21]. In these reports, it was concluded that the radical species formed under UV irradiation was $O_2^{\bullet-}$ (superoxide anion radical) species and that the photocatalytic activity of HAp after treatment at 200 °C (HAp-200) for methyl mercaptane was different from that of HAp after treatment at 1150 °C (HAp-1150). However, the photocatalytic activity of the HAp sample used for dimethyl sulfide (DMS) was not satisfactory under UV irradiation in the previous work. In general, oxidation of DMS is more difficult than that of MM.

In this paper, we describe on a very active type of HAp for photocatalytic decomposition of DMS and the structural characteristics of the material.

2. Experimental

HAp (HAp-1, HAp-2) and β-tricalcium phosphate (TCP) samples were obtained from Sumitomo Osaka Cement Co.

Table 1
Characteristics of HAp and TCP samples

Sample	Ca/P	Surface area ($m^2\,g^{-1}$)
TCP	1.50	42
HAp-1	1.67	60
HAp-2	1.76	43

Ltd. All samples were heated at 200 °C for 1 h. Characteristics of the samples are shown in Table 1.

DMS was purchased from Tokyo Kasei Co. and sample gas was prepared with pure air (Nippon Sanso Co.).

The experimental apparatus for photocatalytic reaction of DMS was described in the previous paper [21]. Photocatalytic reaction of DMS in air was performed at the space velocity of $340\,h^{-1}$. The light source used was UV (254 nm) type (Toshiba Lightec, 6 W). Photocatalytic reaction vessel was covered with aluminum foil to shut off the outside light. DMS in inlet and effluent gas was measured by gas chromatograph (Shimadzu GC-15A) equipped with flame photometric detector. SO_2 in effluent gas was measured by a Japan Thermoelectron Model 43C analyzer. CO_2 was measured by gas chromatograph (Hitachi GC-663) equipped with methanyzer followed by flame ionization detector.

X-ray diffraction (XRD) patterns were recorded on a Rigaku Multiflex diffractometer using Cu Kα radiation. Fourier transform infrared (FTIR) spectra were measured with a JASCO Hershel FTIR-480 equipped with an infrared microscope Irtron IRT-30. Electron spin resonance spectra were recorded on a JEOL JES-FA200 spectrometer. Radical species were detected as spin adducts and the spin trapping reagent used was 5,5-dimethyl-1-pyrroline-1-oxide (DMPO). The ESR spectrometry conditions were as follows: magnetic field: 323.3 mT; power: 4 mW, 9.06 GHz; sweep time: 30 s; modulation: 100 kHz, 0.35 mT; amplitude: 100; time constant: 0.03 s. BET surface area was measured with a Micromeritics Autopore 9200 at 77 K.

3. Results and discussion

3.1. Comparison of photocatalytic decomposition for DMS among HAp and TCP samples

The photocatalytic decomposition efficiencies of DMS under UV irradiation for HAp-1, HAp-2 and TCP were investigated. The results are shown in Fig. 1. Photocatalytic decomposition of DMS scarcely occurred in blank test. The conversion of DMS using TCP was under 45% and the conversion using HAp-1 was 74–78%. On the other hand, the conversion using HAp-2 was 98–100%. The photocatalytic activity of HAp-2 for DMS was found to be very high. The activity could not be due to the surface area because the BET surface area of HAp-2 was smaller than that of HAp-1 as shown in Table 1.
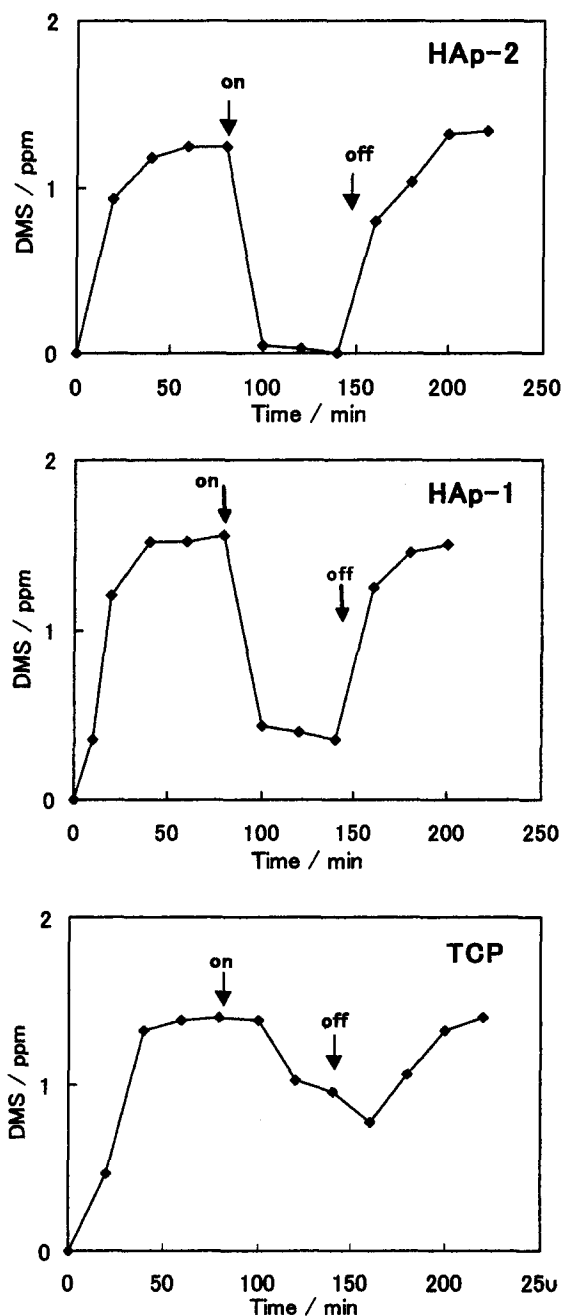

Fig. 1. Photocatalytic decomposition of DMS using three types of materials.

The continuous photocatalytic decomposition of low levels of DMS over HAp-2 under UV irradiation is shown in Fig. 2. The conversion of DMS remained almost 100% from 90 min after lighting. The concentration levels of DMS tested are the maximum levels of usual existing in the actual emission or atmosphere. It was recognized that HAp-2 was very effective for the photocatalytic decomposition of DMS.

3.2. Reaction process

To investigate the photocatalytic reaction of DMS over HAp-2, high concentration of DMS (92 ppm (v/v)) in air
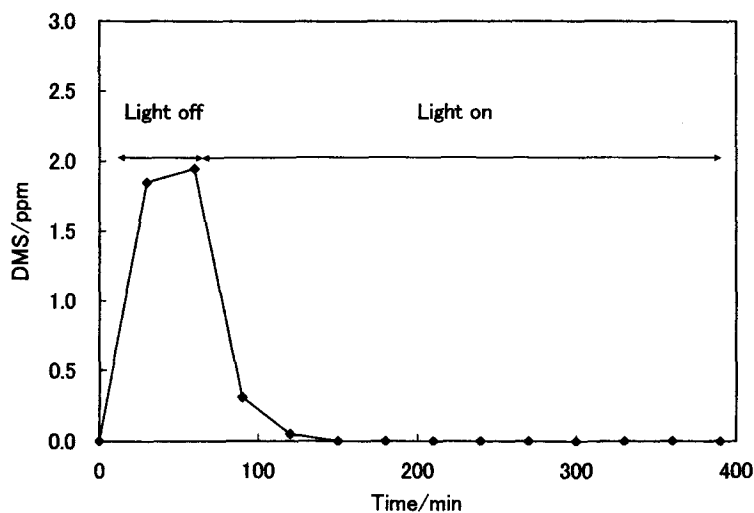
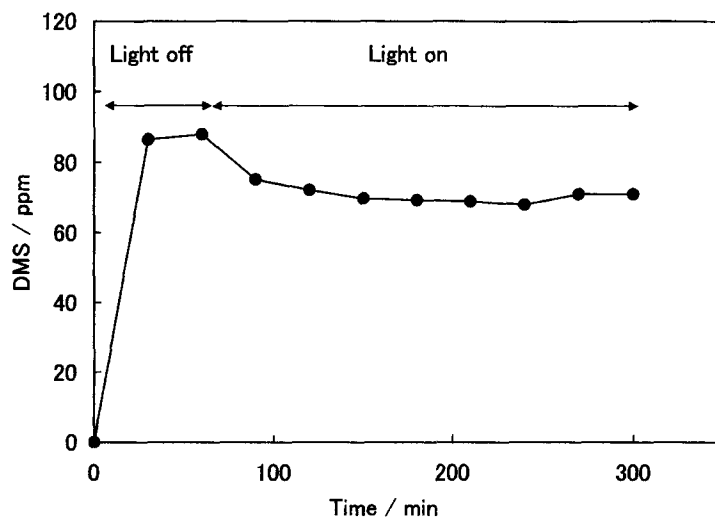Fig. 2. Continuous photocatalytic decomposition of low concentrations of DMS over HAp-2.


Fig. 3. Continuous photocatalytic decomposition of high concentrations of DMS over HAp-2.

was used to test. The results are shown in Fig. 3 and Table 2.

The average conversion of DMS was 28% under the condition. The selectivities of SO_2 and CO_2 calculated from the concentrations detected in outlet gas were 0.04 and 102%, respectively. DMDS was not found in decomposed gas. That is, C in the reacted DMS molecule was completely converted to CO_2. It is known that major parts of SO_2 produced by the reaction are adsorbed by the HAp sample as described in previous paper [21]. These results show that the photocat-

Table 2
Decomposition of DMS on HAp-2 under UV irradiation

Conversion of DMS (%)	Selectivities of the compounds in decomposed gas		
	DMDS (%)	SO_2 (%)	CO_2 (%)
28	0	0.04	102

DMS in inlet: 92 ppm (v/v); space velocity: $340\,h^{-1}$.

alytic oxidation proceeds very effectively and stoichiometrically in the reaction. The oxidative reaction would proceed on HAp under UV irradiation as follows:

$$2CH_3SCH_3 + 9O_2 \rightarrow 4CO_2 + 2SO_2 + 6H_2O$$
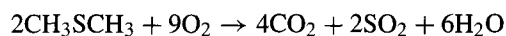
3.3. FTIR and XRD studies

FTIR spectra and XRD patterns of HAp-1 and HAp-2 were measured to investigate the structural characteristics of these materials. The FTIR spectra are shown in Fig. 4. The bands due to apatitic OH appear at 3570 and $630\,cm^{-1}$. The broad peaks around 3400 and $1640\,cm^{-1}$ assigned to H_2O liberations. The characteristic bands for PO_4 group appear at around 1030 and $962\,cm^{-1}$. The spectra of HAp-1 almost coincide with those of HAp-2. The structural difference on IR measurement between HAp-1 and HAp-2 was not recognized.
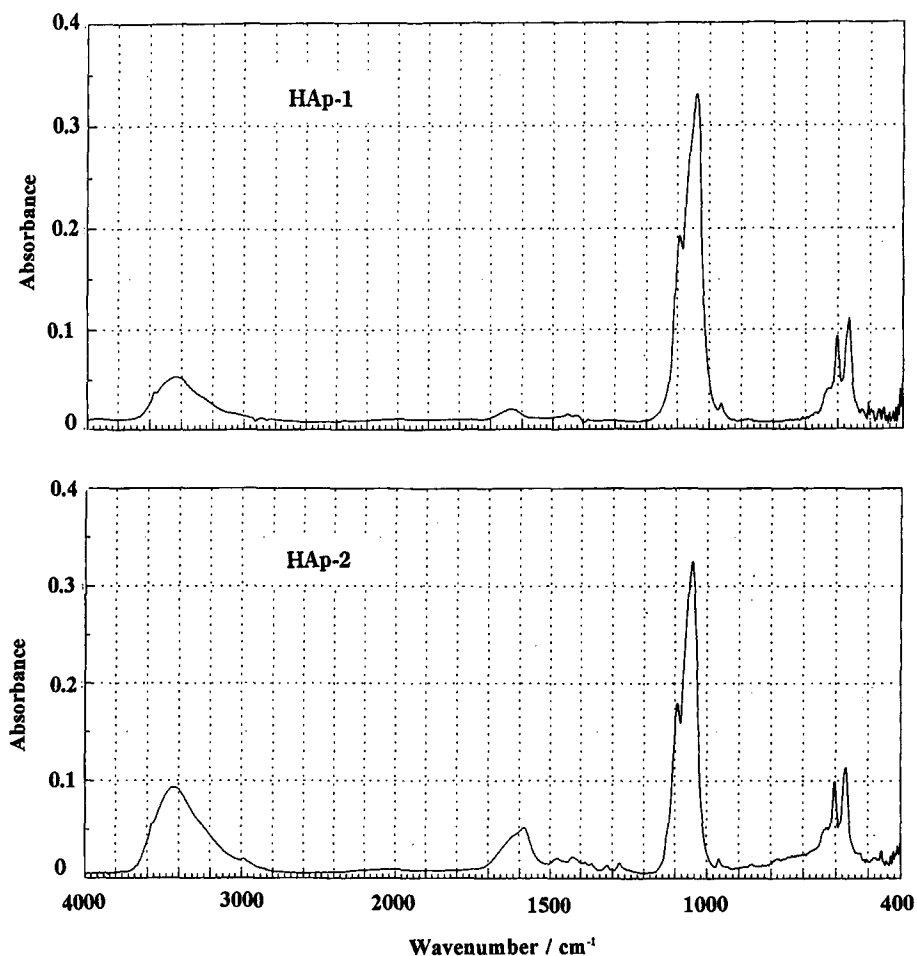
Fig. 4. FTIR spectra of HAp-1 and HAp-2.

The XRD patterns of the HAp samples are shown in Fig. 5. Generally, the broadening of XRD peaks reflects the lowering of crystallinity of the corresponding lattice directions. The crystallinity is influenced by crystal size and disorder. The (3 0 0) peak of HAp-1 broadens compared to that of HAp-2. On the other hand, the (0 0 2) peaks of the two samples have similar sharpness. The results shows that the HAp-1 crystals have a lower crystallinity than crystals of HAp-2 toward the apatite a-axis, but a similar crystallinity toward the c-axis. That is, HAp-2 crystals have a high crystalinity toward the a-axis.

It is recognized that the difference of the catalytic activities in apatite and related compounds could be due to a different disorder of the crystals by Ozaki et al. [22] and our previous works [10]. Ohno et al. [23] found that one crystal face was more oxidative than the other faces in photocatalytic activity of TiO_2 (anatase). From these studies and our results, it is concluded that the photocatalytic activity of HAp in the previous section must be due to the crystallinity toward the a-axis of HAp crystal. Then, HAp-2 would be very active for photocatalytic decomposition of DMS.
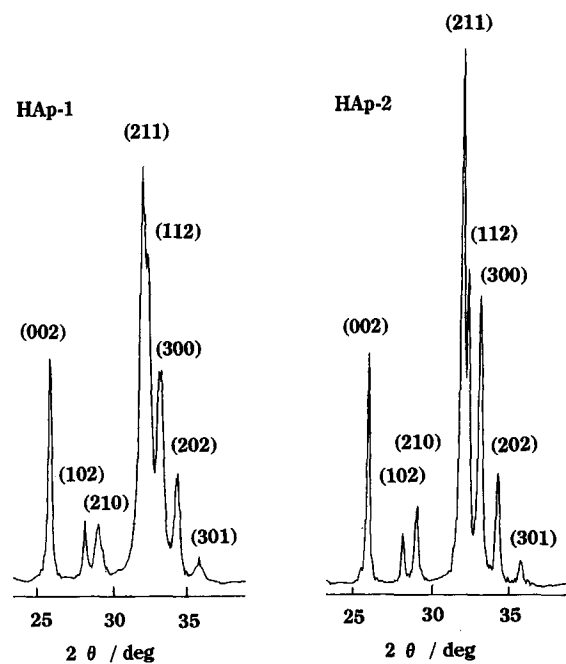

Fig. 5. XRD patterns of HAp-1 and HAp-2.

3.4. Radical formation by ESR study

ESR studies were performed to confirm the generation of active radicals on HAp-1 and HAp-2 by UV irradiation. From the ESR results by the spin trapping method (DMPO/H_2O), the characteristic signals after UV irradiation showed the formation of the DMPO adduct of OH radical on the two HAp samples. That is, the active oxygen radical appeared on the HAp samples by UV irradiation as well as the results described in the previous report [20]. The radical species must contribute effectively to the oxidative decomposition of DMS on HAp.

Acknowledgements

References

[1] J.A.S. Bett, L.G. Christner, W.K. Hall, J. Am. Chem. Soc. 89 (1967) 5535.
[2] H. Monma, J. Catal. 75 (1982) 200.
[3] Y. Izumi, S. Sato, K. Urabe, Chem. Lett., (1983) 1649.
[4] W.T. Reichle, J. Catal. 17 (1970) 297.
[5] N.S. Figoli, H.R. Keselman, P.C. Largentiere, C.L. Lazzaroni, J. Catal. 77 (1982) 64.
[6] N.S. Figoli, C.L. Lazzaroni, H.R. Keselman, P.C. Largentiere, J. Catal. 85 (1984) 538.
[7] H. Nishikawa, H. Monma, Nippon Kagaku Kaishi, (1991) 1562.
[8] H. Nishikawa, S. Ikeda, H. Monma, Bull. Chem. Soc. Jpn. 66 (1993) 2570.
[9] H. Nishikawa, H. Monma, Phos. Res. Bull. 3 (1993) 115.
[10] H. Nishikawa, H. Monma, Bull. Chem. Soc. Jpn. 67 (1994) 2454.
[11] H. Monma, S. Ueno, T. Kanazawa, J. Chem. Tech. Biotechnol. 31 (1981) 15.
[12] Y. Matsumura, H. Kanai, J.B. Moffat, J. Chem. Soc., Faraday Trans. 93 (1997) 4383.
[13] H. Kanai, Y. Matsumura, J.B. Moffat, Phos. Res. Bull. 6 (1996) 293.
[14] P.D. Moens, F.J. Callens, P.F. Matthys, R.M. Verbeeck, J. Chem. Soc., Faraday Trans. 90 (1994) 2653.
[15] G.C.A.M. Vanhaelewyn, R.A. Morent, F.J. Callens, P.F.A.E. Matthys, Radiat. Res. 154 (2000) 467.
[16] P. Moens, F. Callens, S. Van Doorslaer, P. Matthys, Phys. Rev. B 53 (1996) 5190.
[17] D.U. Schramm, A.M. Rossi, Phys. Chem. Chem. Phys. 1 (1999) 2007.
[18] D.U. Schramm, A.M. Rossi, Appl. Radiat. Isot. 52 (2000) 1085.
[19] T. Murata, K. Shiraishi, Y. Ebina, T. Miki, Appl. Radiat. Isot. 47 (1996) 1527.
[20] H. Nishikawa, Mater. Lett. 50 (2001) 364.
[21] H. Nishikawa, K. Omamiuda, J. Mol. Catal. A Chem. 179 (2002) 193.
[22] K. Ozaki, M. Doi, T. Kanesaka, I. Matuura, Proceedings of the 72nd Conference, Shokubai Toronkai (A), 1993, p. 454.
[23] T. Ohno, K. Sarukawa, M. Matsumura, New J. Chem. 26 (2002) 1167.